Supplementary information

An Insight into Sensitive detection of Metal ions using a Novel Cobalt MOF: Single crystal, Photoluminescence, and theoretical studies

Love Karan Rana[1], Prabhjyot Kaur[1], Thierry Maris[2], and Adam Duong[1]*

Table of contents

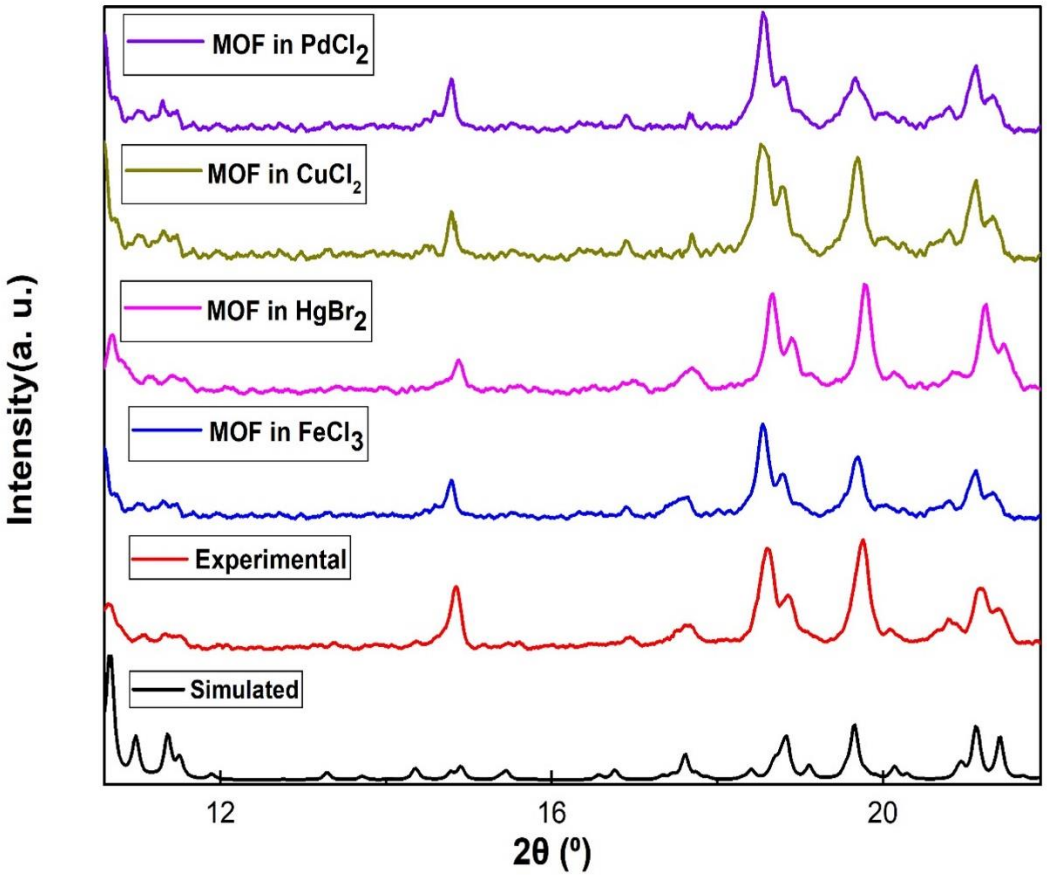

Fig. S1- Comparison of PXRD pattern of asynthesized compound **1** and patterns recorded after exposing **1** to different metal ions solutions with the simulated pattern.(Here compound **1** has been denoted as MOF for the illustration to be meaningful).

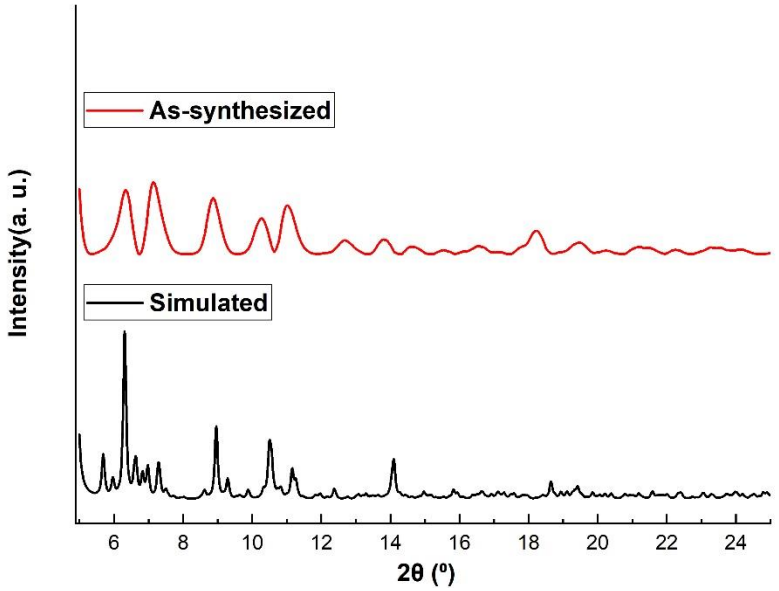

Fig. S2- Comparison of PXRD pattern of asynthesized compound **2** and its simulated pattern.

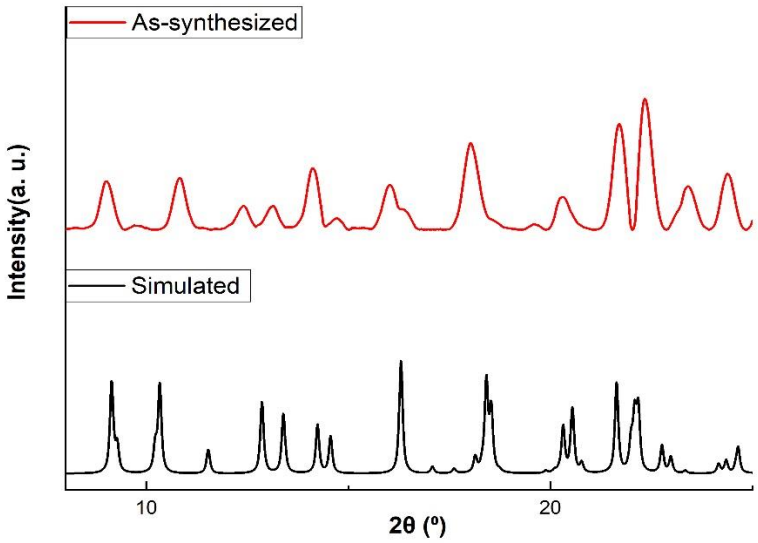

Fig. S3- Comparison of PXRD pattern of asynthesized compound **3** and its simulated pattern.

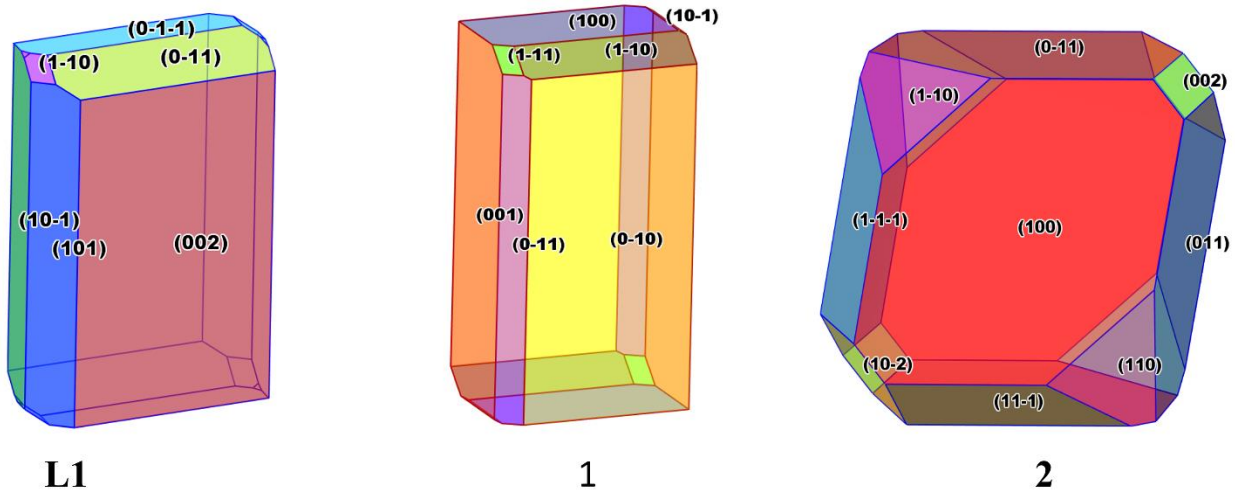

Fig. S4- BFDH morphologies of **L1**, compound **1** and **2**.

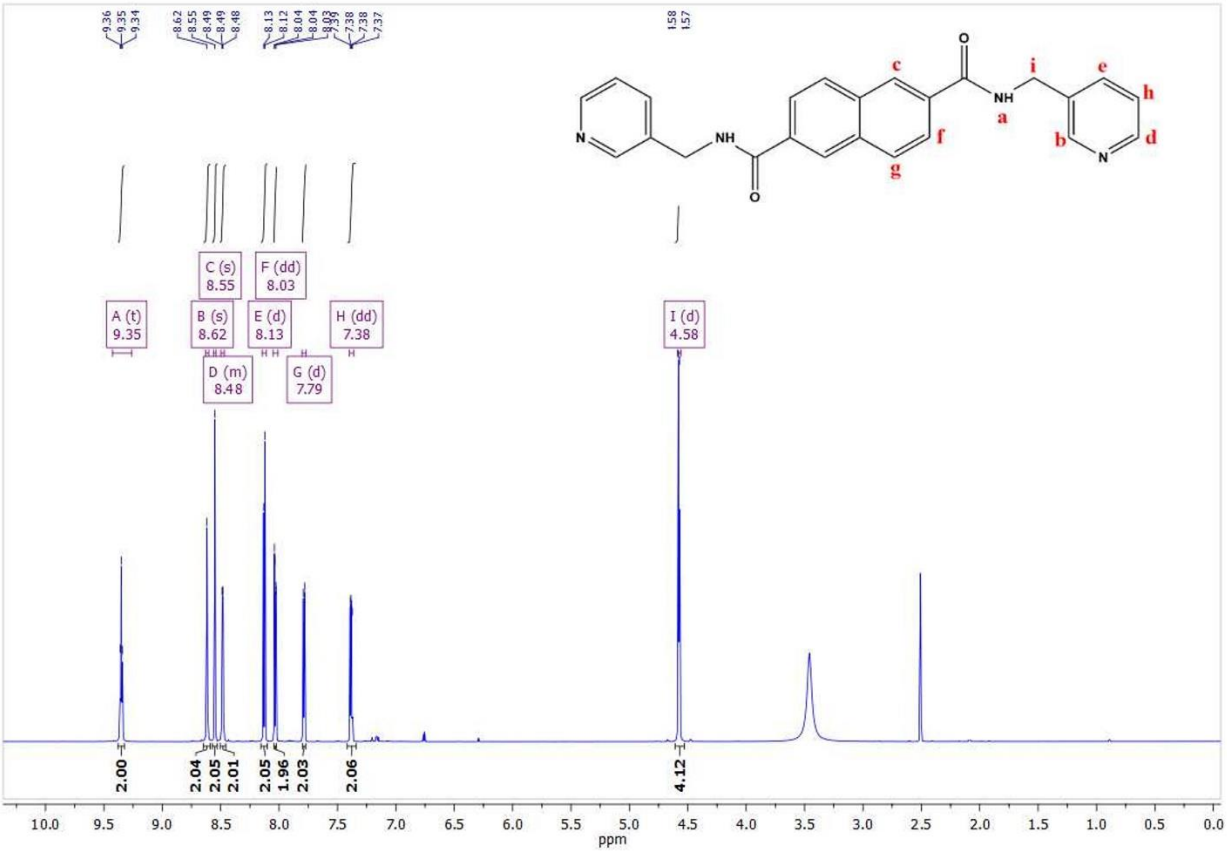

Fig. S5 ^{1}H-NMR of **L1**

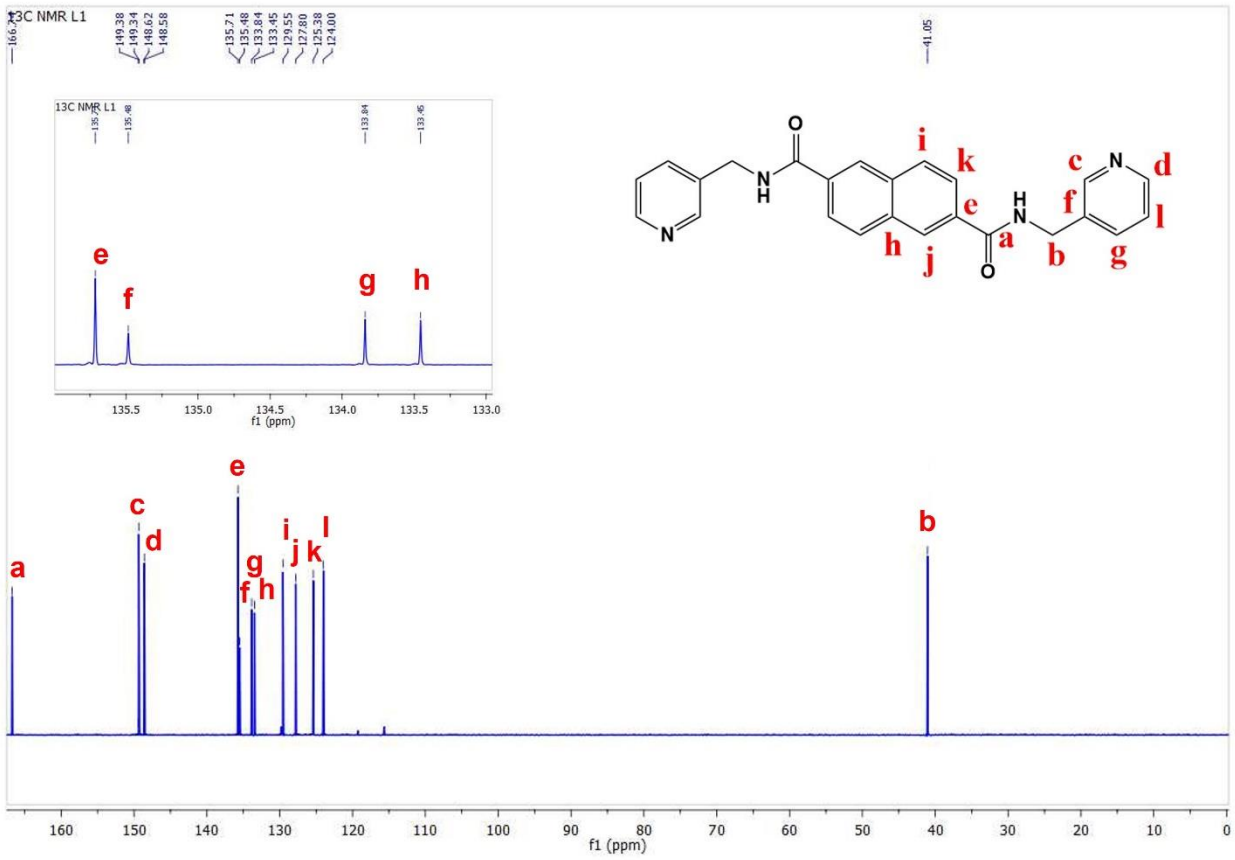

Fig. S6 ^{13}C-NMR of **L1**

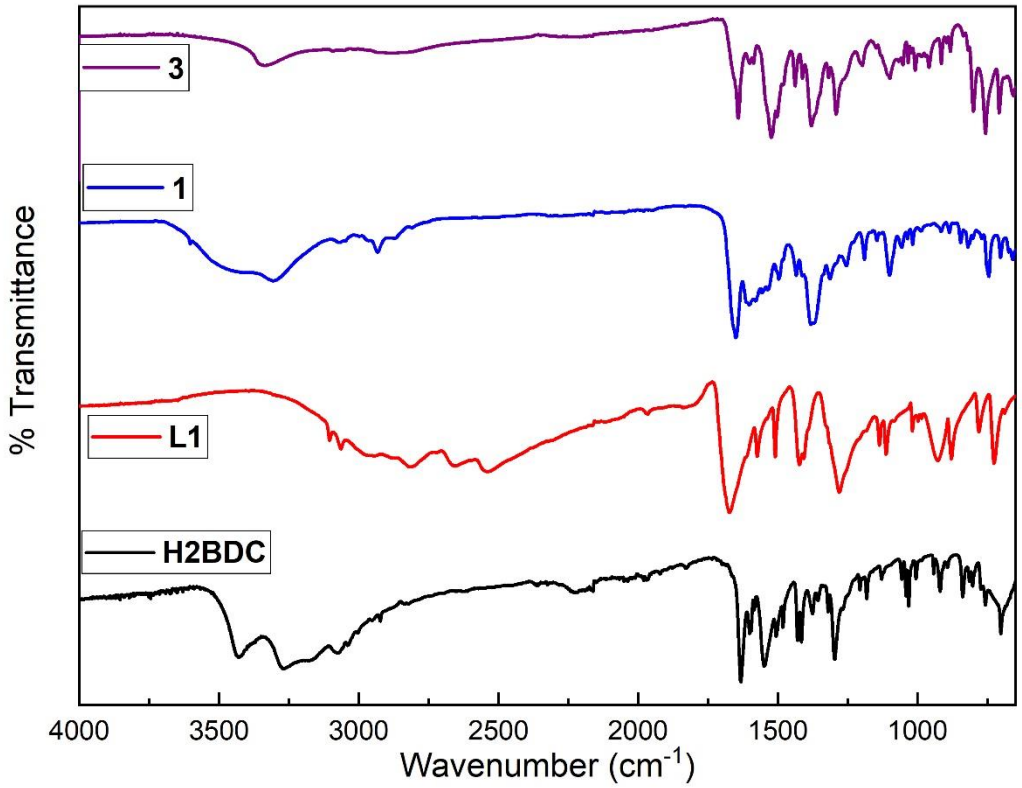

Fig. S7 – IR spectra comparison of **L1**, **H2BDC**, and compound **1** and **3**.

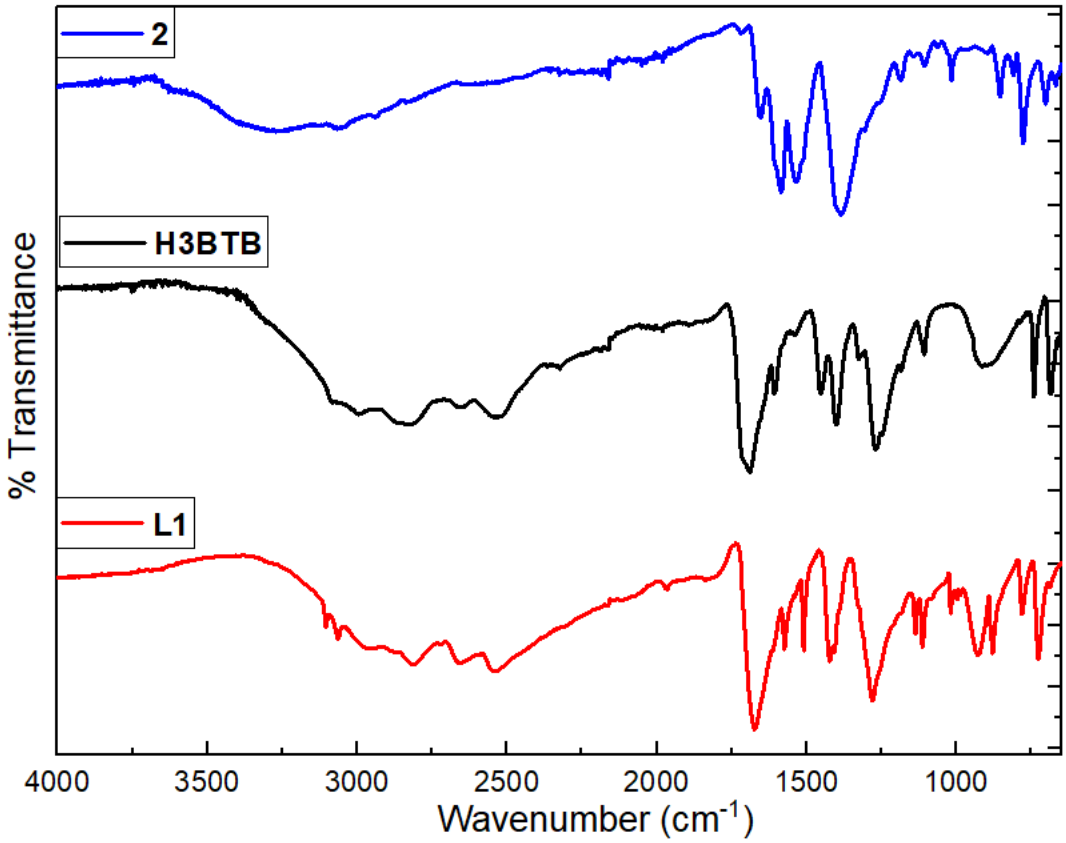

Fig. S8 – IR spectra comparison of **L1**, **H3BTB**, and compound **2**.

From the IR spectra (Fig. S7) it is apparent that the peak at 1509 and 1574 cm^{-1} (C=N stretching, pyridine ring) in **L1** (Red graph) slightly shifted in the spectra of compound **1** (blue graph) confirming the coordination of pyridine rings to Co(II) ions, while the peak at 1673cm^{-1} corresponds to C=O stretching of **L1** (amide group, red graph) is slightly shifted in **1** (1652cm^{-1}) which might be due to the hydrogen bonding with solvent molecules (DMF) (Fig. S7). Similarly, the peak at 1631cm^{-1} (C=O stretching, carboxylic group) in **H2BDC** (black graph) is shifted and flattened at 1616 cm^{-1} in the spectra of **1** (blue graph) which confirms the coordination of carboxylic groups to Co(II) ions (Fig. S7). In the case of **3**, respective spectral peaks confirms the coordination of ligands with Ni(II). In addition, a sharp band at 1523 cm^{-1} and a weak band at 1593 cm^{-1}, respectively, confirms the presence both free and coordinated carbonyl groups (carboxylic) (Fig. S7). A shift of 16 cm^{-1} (from 1676 cm^{-1} (**L1**) to 1660 cm^{-1}) in **2** (Fig. S8**)** was observed for C=O (amide) stretching, which might be due the hydrogen bonding between amide group and

lattice DMF molecules. Similarly, an observed shift in N-H (amide group) stretching frequency from 3104 cm^{-1} (**L1**) to 3061 cm^{-1} (**2**) is due to hydrogen bonding with DMF molecules.

Table S1- IR table

Complex	Group	Functionality	Wavenumber (cm^{-1})
L1	ν (N-H)	Amide	3105 (m, s)
	ν (C=O)	Amide	1667(s)
	ν (C=N)	Pyridine	1510 (m,s)
	ν $(C-H)_{bending}$	Naphthalene	1417 (m, s)
1	ν (N-H)	Amide	3286 (b)
	ν (C=O)	Amide	1652 (s)
	ν (C=N)	Pyridine	1491 (w)
	ν $(C-H)_{bending}$	Naphthalene	1378 (m, s)
	ν (C-H) $_{Overtone}$	Naphthalene	2870 (w)
	ν (C-H)	Methyl group (DMF)	2929 (w)
2	ν (N-H)	Amide	3095 (w, b)
	ν (C=O)	Amide	1662 (m)
	ν (C=O)	Carboxylic	1590 (m, s)
3	ν (N-H)	Amide	3335 (b)
	ν (C=O)	Amide	1641 (m, s)
	ν $(C=O)_{free}$	Carboxylic	1523 (s)
	ν $(C=O)_{Coordinated}$	Carboxylic	1593 (m, w)

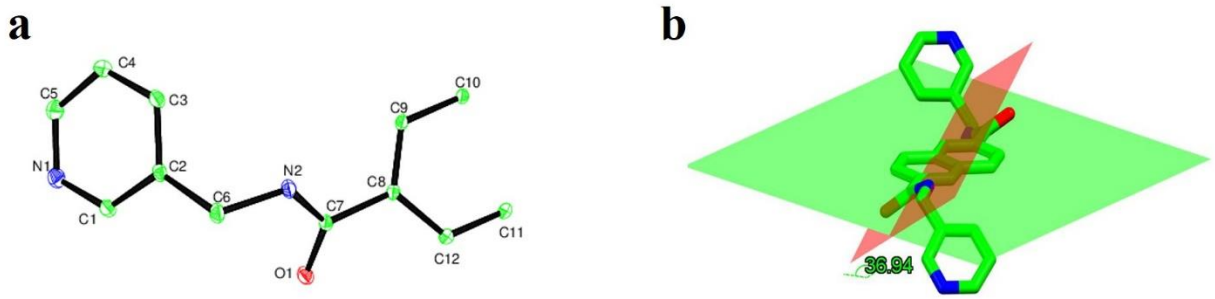

Fig. S9 a) ORTEP diagram of **L1** at 30% probability, b) showing dihedral angle between naphthalene and amide plane.

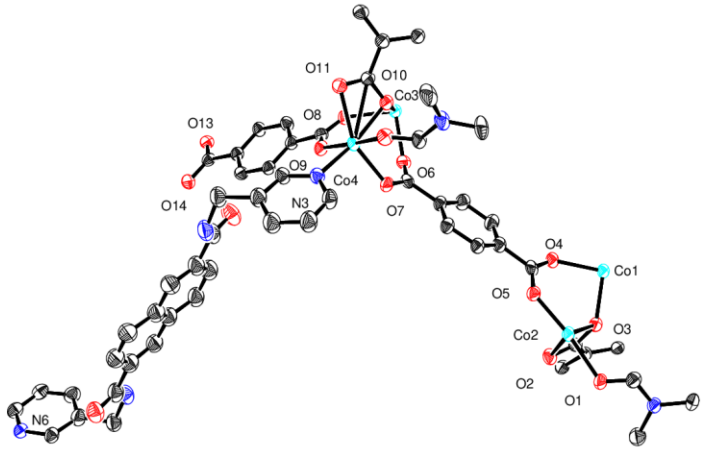

Fig. S10 ORTEP diagram of **1** at 30% probability.

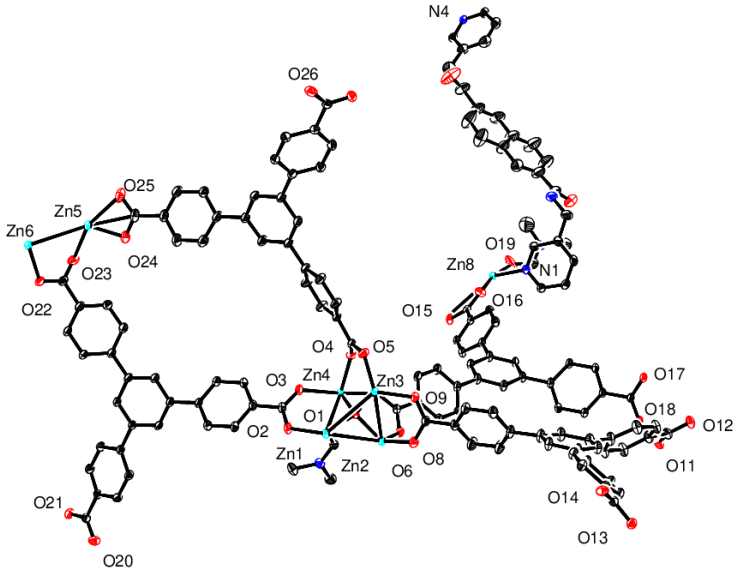

Fig. S11 ORTEP diagram of **2** at 30% probability.

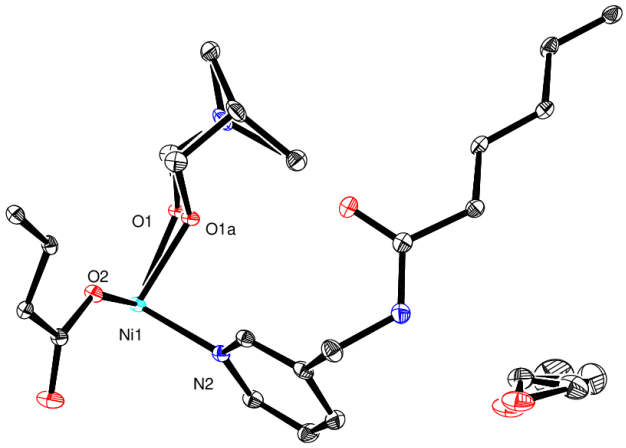

Fig. S12 ORTEP diagram of **3** at 30% probability.

Thermal stability-

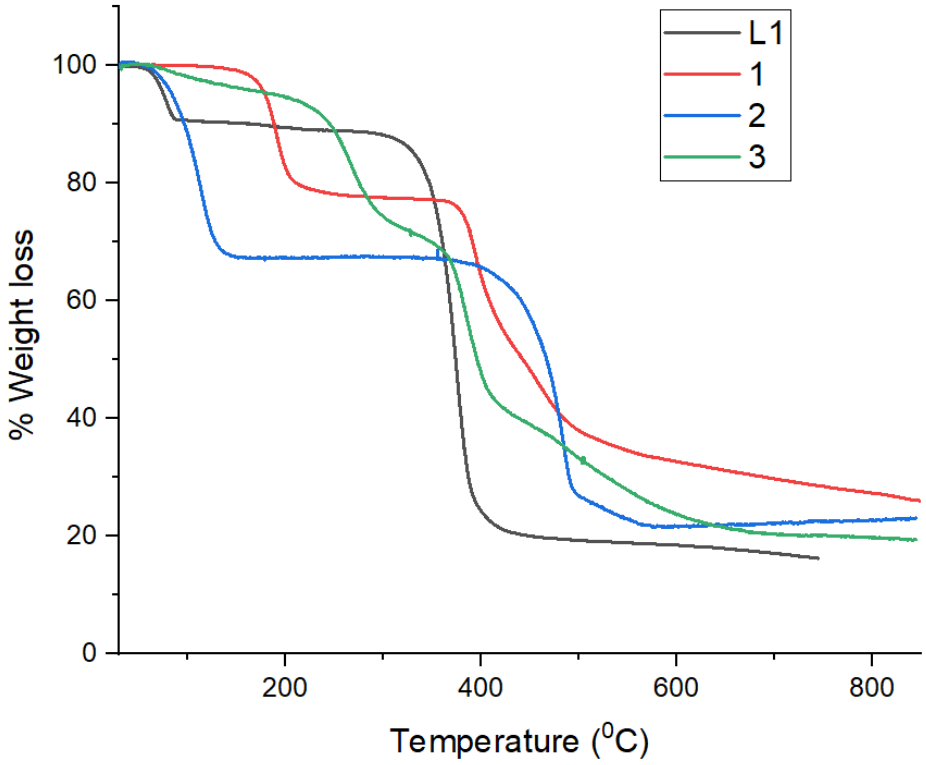

Fig. S13 Thermal stability curves of **L1,** compound **1**, **2**, and **3**.

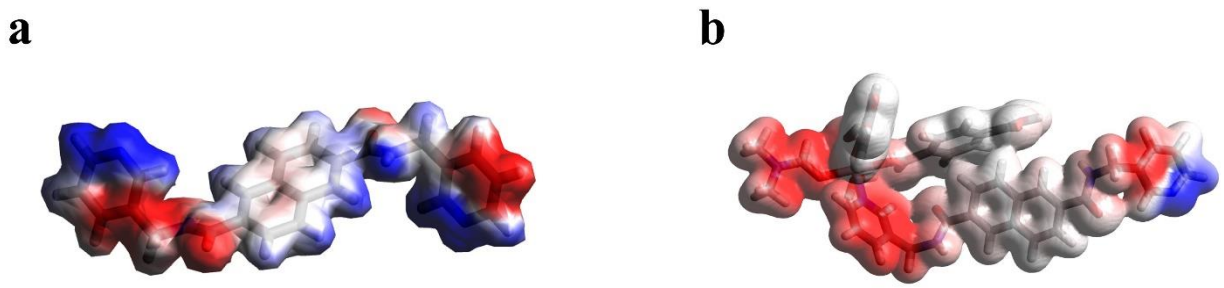

Fig. S14 - Electrostatic potentials mapped on electron isodensity surface at 0.01 au. MEP plot a) for **L1**, and b) Co(II) complex using Avogadro software[1]. (RWB scheme was used, where red colour corresponds to high electron density regions and blue colour corresponds to least electron density regions)

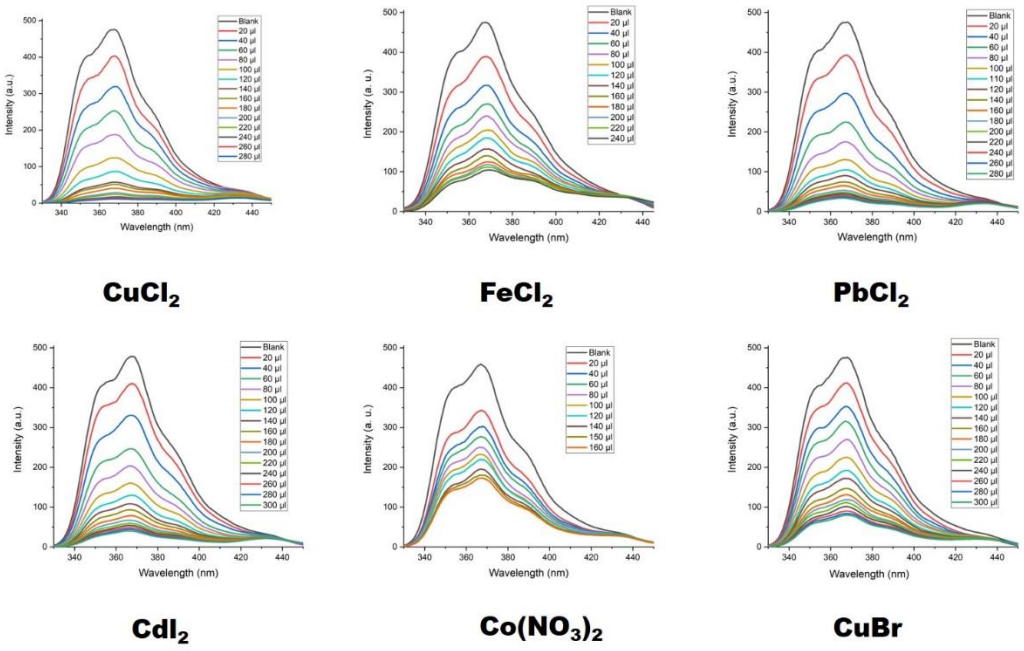

Fig. S15 Quenching of fluorescence intensity of **1** by Cu^{+2}, Fe^{+2}, Pb^{+2}, Cd^{+2}, Co^{+2}, and Cu^{+} ions. (Note- Blank corresponds to the emission from **1** before the addition of analytes)

Stern-Volmer plots

Stern-Volmer equation is used to find out the catalytic efficiency of analytes in a photophysical intermolecular deactivation process. The equation is $(I_0/I) = K_{SV}[A] + 1$, where in our case, I_0 is the initial fluorescence intensity of **1** soaked in DMF, I is the fluorescence intensity in the presence of analyte, [A] is the molar concentration of analyte, and K_{SV} is the Stern-Volmer constant (M^{-1}) or quenching constant.

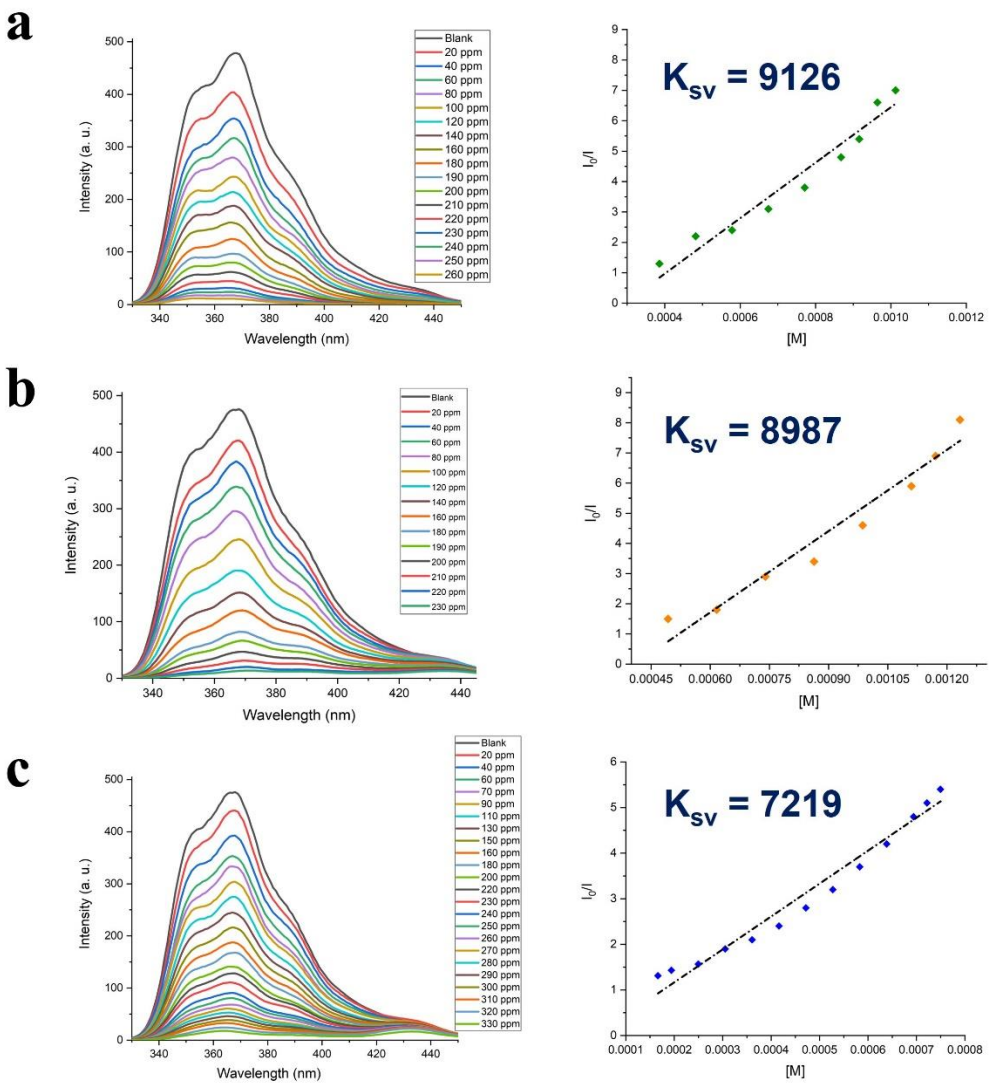

Fig. S16- Emission spectra and the corresponding Stern-Volmer plots of **1** in different **a)** Ru^{+3}, **b)** Fe^{+3} and **c)** Hg^{+2} concentrations in DMF.

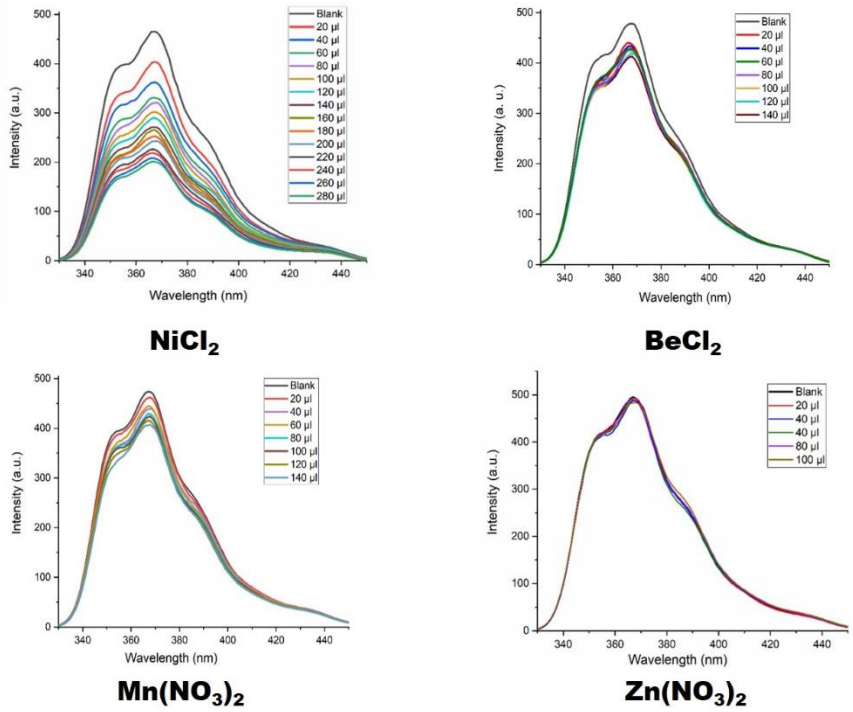

Fig. S17 Quenching of fluorescence of **1** by Ni^{+2}, Be^{+2}, Mn^{+2}, and Zn^{+2} ions. (Note- Blank corresponds to the emission from **1** before the addition of analytes)

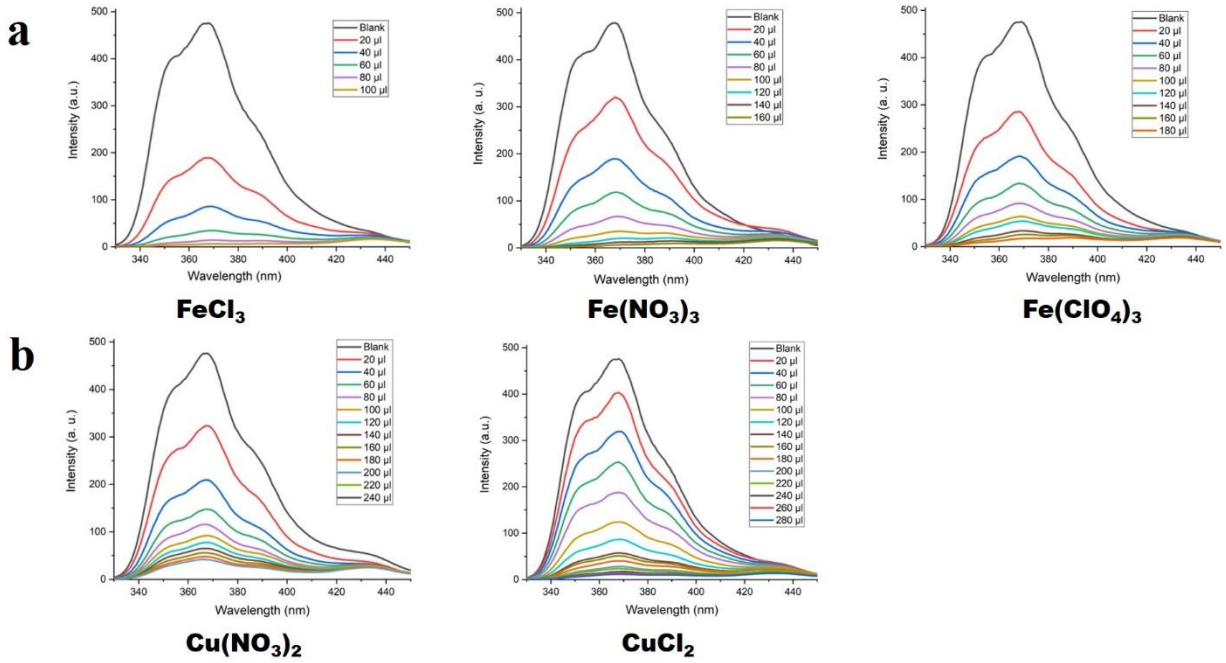

Fig. S18 Comparison of fluorescence quenching of **1** with **a)** different Fe(III) and **b)** Cu(II) salts. (Note- Blank corresponds to the emission from Co-MOF before the addition of analytes)

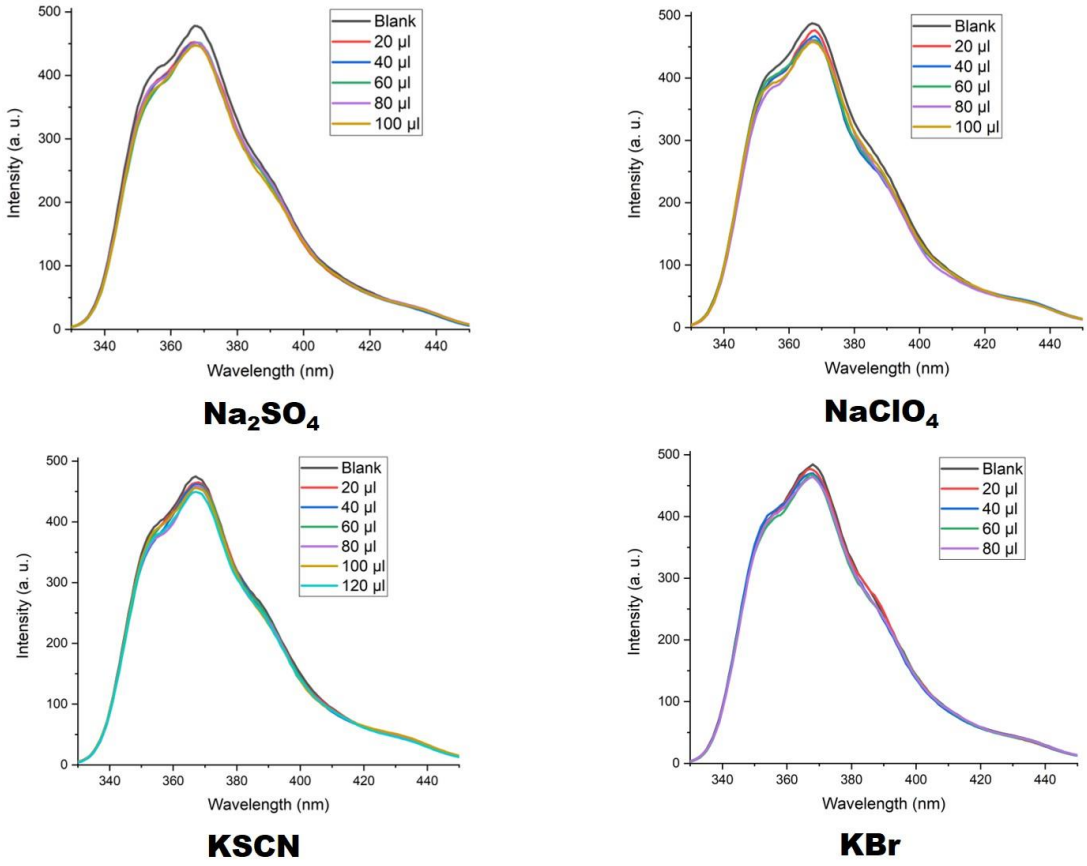

Fig. S19 Illustrates negligible change in fluorescence intensity upon the addition of ClO_4^-, SCN^-, and Br^- ions. (Note- Blank corresponds to the emission from **1** before the addition of analytes)

Table S2- Pertinent atomic parameters for compound **1**, **2**, and **3.**

Bond lengths		
1	**2**	**3**
Co4-N3 2.150(10)	Zn1-O1 1.919(2)	Ni1-N2 2.118(2)
Co2-N6^4 2.141(10)	Zn1-O2 1.908(2)	Ni1-O1 2.072(15)
Co1-O3^1 2.127(7)	Zn1-O14^1 1.983(2)	Ni1-O2^3 2.0420(18)
Co1-O4 2.048(7)	Zn1-O21^2 1.960(2)	
Co1-O13^2 2.066(6)	Zn2-O1 1.927(2)	
Co1-O13^3 2.066(6)	Zn2-O6 1.935(2	
Co2-O1 2.154(7)	Zn2-O8 1.980(2)	
Co2-O2 2.237(7)	Zn2-O13^1 1.960(2)	
Co2-O3 2.140(7)	Zn3-O1 1.929(2)	
Co2-O5 2.021(7)	Zn3-O5 1.927(2)	

Co2-O14[3] 2.034(6)	Zn3-O9 1.959(2)	
Co3-O6 2.069(7)	Zn3-O20[2] 1.977(2)	
Co3-O8[5] 2.054(6)	Zn4-O1 2.030(2)	
Co3-O10[5] 2.116(7)	Zn4-O3 2.198(2)	
Co4-O7 2.047(7)	Zn4-O4 2.122(2)	
Co4-O9 2.021(6)	Zn4-O7 2.112(2)	
Co4-O10 2.140(8)	Zn4-O10 2.135(2)	
Co4-O11 2.261(7)	Zn4-N4[3] 2.102(3)	
Co4-O12 2.135(6)	Zn5-O9[4] 1.951(2)	
	Zn5-O23 2.020(3)	
	Zn5-O24 1.952(3)	
	Zn5-O25 2.384(3)	
	Zn5-O27[5] 1.965(3)	
	Zn6-O9[4] 1.952(2)	
	Zn6-O11[6] 1.959(3)	
	Zn6-O18[6] 1.974(2	
	Zn6-O22 1.951(2)	
	Zn7-O9 1.925(2)	
	Zn7-O15 1.924(2)	
	Zn7-O17[5] 1.961(2)	
	Zn7-O26[7] 1.954(3)	
	Zn8-O9 1.953(2)	
	Zn8-O12[5] 1.977(2)	
	Zn8-O16 2.043(3)	
	Zn8-O19 2.272(4)	
	Zn8-N1 2.031(3)	
Bond angles		
O3-Co1-O3[1] 180	O1-Zn1-O14[1] 108.56(9)	O1[3]-Ni1-N2 85.3(6)
O4-Co1-O3 92.2(3)	O1-Zn1-O21[2] 111.96(10)	O1-Ni1-N2 94.7(6)
O4-Co1-O3[1] 92.2(3)	O2-Zn1-O1 122.81(9)	O1A[3]-Ni1-O1A 180.00(17)
O4-Co1-O3[1] 87.8(3)	O2-Zn1-O14[1] 102.98(11)	O1A[3]-Ni1-N2[3] 85.32(14)
O4-Co1-O4 180.0(4)	O2-Zn1-O21[2] 106.50(11)	O1A[3] -Ni1-N2 94.68(14)
O4-Co1-O13[2] 85.8(3)	O21[2]-Zn1-O14[1] 101.72(11)	N2-Ni1-N2[3] 180.0
O4-Co1-O13[3] 94.2(3)	O1-Zn2-O6 115.29(9)	O2-Ni1-O1[3] 90.5(7)
O13[2]-Co1-O3[1] 87.9(3)	O1-Zn2-O8 109.39(10)	O2-Ni1-O1[3] 89.5(7)
O13[3]-Co1-O3[1] 92.1(3)	O1-Zn2-O13[1] 113.61(9)	O2[3]-Ni1-O1A 91.05(18)
O13[2]-Co1-O13[3] 180.0	O6-Zn2-O8 101.04(11)	O2[3]-Ni1-O1A[3] 88.95(18)
O1-Co2-O2 82.9(3)	O6-Zn2-O13[1] 105.44(11)	O2-Ni1-N2 90.61(8)
O3-Co2-O1 84.0(3)	O13-Zn2-O8 111.37(10)	O2-Ni1-N2[3] 89.39(8)
O3-Co2-O2 59.6(3)	O1-Zn3-O9 112.64(11)	O2-Ni1-O2[3] 180
O3-Co2-N6[4] 162.5(3)	O1-Zn3-O20[2] 108.15(10)	
O5-Co2-O1 173.3(3)	O5-Zn3-O1 116.65(9)	
O5-Co2-O2 95.1(3)	O5-Zn3-O9 113.75(11)	
O5-Co2-O3 100.5(3)	O5-Zn3-O20[2] 108.01(12)	
O5-Co2-O14[3] 98.8(3)	O9-Zn3-O20 95.17(12)	
O5-Co2-N6[4] 88.3(3)	O1-Zn4-O3 93.19(8)	
O14[3]-Co2-O1 85.5(3)	O1 -Zn4-O4 92.69(9)	
O1-Co2-O2 153.9(3)	O1-Zn4-O7 94.01(9)	
O14[3]-Co2-O3 96.1(3)	O1-Zn4-O10 88.67(9)	
O14[3]-Co2-N6[4] 97.5(3)	O1-Zn4-N4 178.66(10)	

N6^{4}-Co2-O1 86.1(3) N6^{4}-Co2-O2 104.9(3) O6-Co3-O6 180.0(3) O6-Co3-O10^{5} 91.4(3) O6^{5}-Co3-O10^{5} 88.6(3) O6-Co3-O10 88.6(3) O6-Co3-O10 91.4(3) O8^{5}-Co3-O6 85.5(3) O8^{5}-Co3 O6^{5} 94.5(3) O8-Co3-O6 94.5(3) O8-Co3-O6^{5} 85.5(3) O8-Co3-O8^{5} 180.0(4) O8-Co3-O10^{5} 91.8(3) O8-Co3-O10^{5} 88.2(3) O8^{5}-Co3-O10^{5} 91.8(3) O8-Co3-O10^{5} 88.2(3) O10-Co3-O10^{5} 180 O7-Co4-O10 97.0(3) O7-Co4-O11 154.8(3) O7-Co4-O12 85.8(3) O7-Co4-N3 94.4(3) O9-Co4-O7 99.1(3) O9-Co4-O10 98.8(3) O9-Co4-O11 93.6(3) O9-Co4-O12 174.3(3) O9-Co4-N3 89.1(3) O10-Co4-O11 59.4(3) O10-Co4-N3 164.9(3) O12-Co4-O10 83.5(3) O12-Co4-O11 83.1(3) O12-Co4-N3 87.5(3) N3-Co4-O11 107.5(3)	O4-Zn4-O3 90.32(9) O4-Zn4-O10 174.61(9) O7-Zn4-O3 172.79(9) O7-Zn4-O4 89.08(10) O7-Zn4-O10 96.03(10) O10-Zn4-O3 84.39(9) N4-Zn4-O3 85.48(10) N4^{3}-Zn4-O4 87.09(10) N4^{3}-Zn4-O7 87.31(10) N4^{3}-Zn4-O10 91.43(10) O9-Zn5-O23 98.71(10) O9^{4}-Zn5-O25 97.20(10) O9^{4}-Zn5-O27^{5} 111.46(10) O23-Zn5-O25 157.89(11) O24-Zn5-O9 132.22(14) O24--Zn5-O23 99.73(13) O24-Zn5-O25 58.16(13) O24-Zn5-O27 110.25(15) O27^{5}-Zn5-O23 95.16(12) O27^{5}-Zn5-O25 93.19(13) O9^{4}-Zn6-O11^{6} 110.98(10) O9^{4}-Zn6-O18^{6} 109.33(9) O11^{6}-Zn6-O18^{6} 101.09(12) O22-Zn6-O9^{4} 119.46(10) O22-Zn6-O11^{6} 107.53(13) O22-Zn6-O18^{6} 106.83(11) O9-Zn7-O17^{5} 110.83(9) O9-Zn7-O26^{8} 114.32(10) O15-Zn7-O9 115.54(9) O15-Zn7-O17^{5} 110.81(10) O15 -Zn7-O26^{8} 107.27(12) O26^{8}-Zn7-O17^{5} 96.44(13) O9-Zn8-O12^{5} 109.75(10) O9-Zn8-O16 98.05(10) O9-Zn8-O19 81.25(12) O9-Zn8-N1 144.95(10) O12-Zn8-O16 97.44(12) O12^{5}-Zn8-O19 93.31(19) O12^{5}-Zn8-N1 102.41(11) O16-Zn8-O19 168.77(18) N1-Zn8-O16 91.10(11) N1-Zn8-O19 83.40(12) Zn1-O1-Zn2 107.90(10) Zn1-O1-Zn3 108.64(10) Zn1-O1-Zn4 109.39(9) Zn2-O1-Zn3 105.78(9) Zn2-O1-Zn4 110.45(10) Zn3 O1 Zn4 114.44(10) Zn5^{7}-O9-Zn6^{7} 108.31(10) Zn5^{7}-O9-Zn8 114.37(10) Zn6^{7}-O9-Zn8 105.06(10)	

	Zn7-O9-Zn5[7] 106.15(10) Zn7-O9-Zn6[7] 108.29(9) Zn7-O9-Zn8 114.41(10)	

Symmetry elements 1: [1]1-X,2-Y,-Z; [2]1-X,2-Y,1-Z; [3]+X,+Y,-1+Z; [4]-X,1-Y,1-Z; [5]2-X,2-Y,1-Z; [6]+X,+Y,1+Z; [7]-X,2-Y,-Z; [8]3-X,2-Y,1-Z. **2:** [1]+X,-1/2-Y,1/2+Z; [2]+X,-1/2-Y,-1/2+Z; [3]1-X,1-Y,1-Z; [4]1+X,1/2-Y,1/2+Z; [5]+X,1/2-Y,1/2+Z; [6]1+X,+Y,1+Z; [7]-1+X,+Y,+Z. **3:** [1]2-X,1-Y,2-Z; [2]2-X,-Y,-Z; [3]1-X,1-Y,1-Z.

References –

1. M. D. Hanwell, D. E. Curtis, D. C. Lonie, T. Vandermeersch, E. Zurek and G. R. Hutchison, *Journal of Cheminformatics*, 2012, DOI:10.1186/1758-2946-4-17.